Concentration and viability measurement of canine stromal vascular fractions using Cellometer.

Introduction

The use of mesenchymal stem cells (MSCs) in regenerative medicine holds great promise for tissues damaged by a number of acute conditions, such as injuries to tendons, ligaments, bone or cartilage and for chronic conditions such as osteoarthritis. MSCs obtained from the stromal vascular fraction (SVF) of adipose tissue, possess multi-lineage differentiation capacity, which allows them to develop into a variety of cell types, including chondrocytes, osteoblasts, myocytes cells and others [1-11]. Accurate determination of cell concentrations and viability in freshly isolated adipose SVF is critical in order to achieve the expected basic or clinical research outcomes.

Cell concentration and viability of SVF preparations are usually determined by standard hemocytometer methods that are prone to considerable error since the operator must make judgments between actual cells versus “debris”. To address that problem, we employed Cellometer® image cytometry to perform both brightfield and fluorescence-based cell concentration and viability measurements [12]. Here, we validated this method for SVF analysis. First, the imaging parameters were optimized by measuring five adipose SVF samples. Next, the concentration and viability of three freshly prepared SVF cell samples were measured and compared using hemocytometer, flow cytometer, and image cytometer methods using trypan blue (TB) and a mixture of Hoechst 33342 and propidium iodide (HO/PI). In addition, a mixture of acridine orange and propidium iodide (AO/PI) was used to measure concentration and viability for the image cytometry method

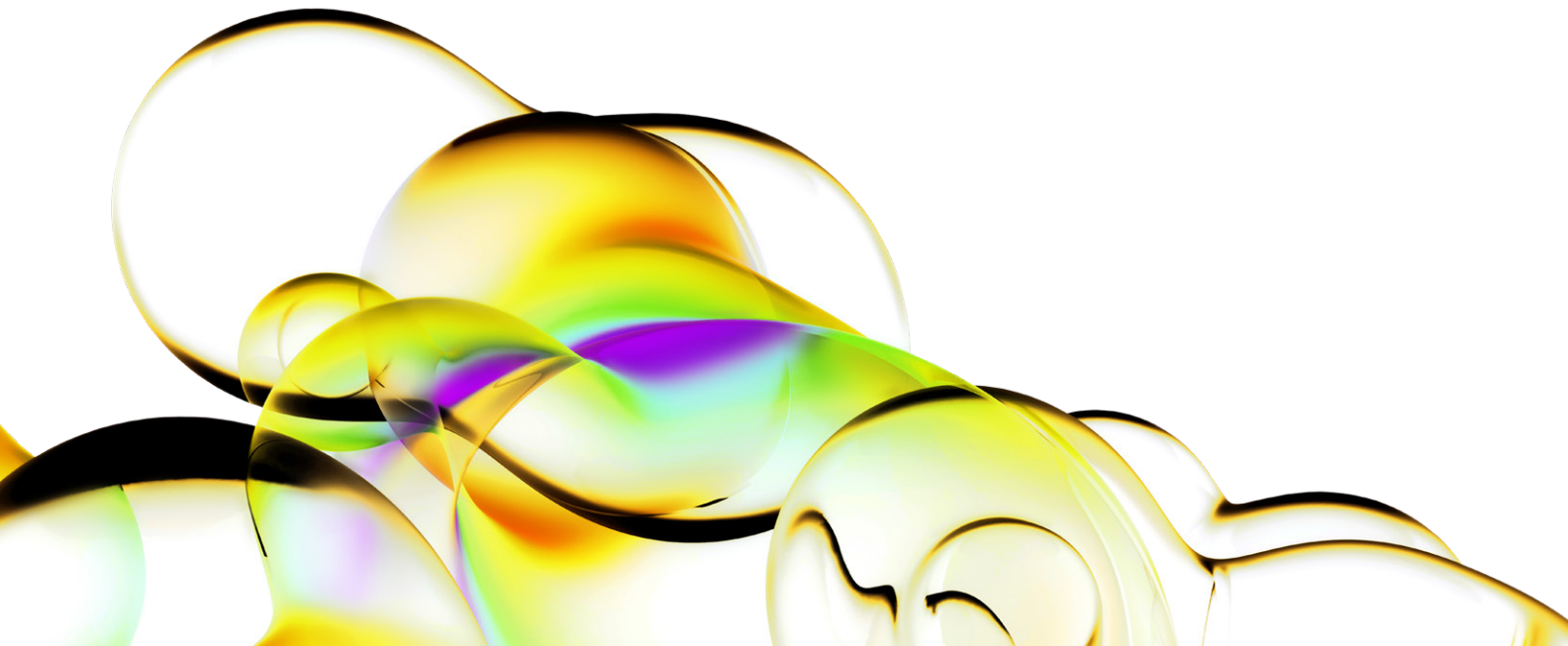

for comparison to HO/PI. The results show comparable concentration measurements amongst the detection methods used, and show that automated image-based cytometry can be used to efficiently generate accurate SVF measurements.

Materials and methods

SVF sample preparation

Stromal vascular fractions (SVF) were collected from canine adipose tissue of individual subjects, using proprietary methods. The SVF samples were transported on ice for analysis within 2 h of tissue processing. Within 1 h of sample receipt, each sample was initially stained with trypan blue (TB) and counted manually on a hemocytometer using standard procedures. The same samples were then analyzed by flow cytometry and image cytometry approaches. Initially, only concentrations of five independent samples (A–E) were measured and compared between flow cytometry, image cytometry, and hemocytometer, in order to validate the Cellometer image cytometry concentration method. Next, both viability and concentrations were compared for two more individual samples (1–2), in order to validate the Cellometer image cytometry viability method.

Hemocytometer protocol

Fresh SVF samples were diluted and subsequently mixed with TB to yield a final concentration. The average of two full squares was used to calculate the percentage viable and dead cells per mL of the SVF sample. The method was performed for the first five samples and then the two individual samples. Manual counting by a Neubauer hemocytometer was performed on four replicate dilutions for each sample and the mean +/– standard deviation was determined.

Cellometer image cytometry protocol

Fresh SVF samples were diluted in PBS. Diluted SVF was stained with AO/PI dual-staining solution and HO/PI solution. The HO/PI staining solution was mixed with cell sample and incubated in the dark for 45 min in a 37 °C water bath before image cytometric analysis. Twenty microliters of sample was mixed uniformly with AO/PI and immediately pipetted into a counting chamber. The counting chamber was then inserted into the image cytometer for automated image analysis. Brightfield and fluorescent images were captured at four different locations, where the AO/PI and HO/PI fluorescent images were counted to determine the live and dead cell count in the sample. The cell size parameters were setup to count only nucleated cells and not the cell debris (4–50 µm). Next, fluorescence thresholds were setup to count only fluorescent positive cells stained with AO, HO, and PI. The AO/PI method was performed for the five optimization samples to measure concentrations. Both AO/PI and HO/PI were performed to compare multiple concentration and viability methods using the final two individual samples. The concentration and viability measurements were performed in quadruplicate.

The Cellometer software utilized the Fluorescence 1 and Fluorescence 2 imaging mode to generate cell counts for live cells (AO- and HO-positive) and dead cells (PI-positive). The cell counts were then used to automatically generate concentration and viability data. Cellometer image cytometer was used for SVF measurement using fluorescence optics modules (FOMs) VB-535-402 (EX: 470 nm, EM: 535 nm), VB-450-302 (EX: 375 nm, EM: 450 nm), and VB-660-502 (EX: 540 nm, EM: 660 nm) for AO, HO, and PI detection, respectively. The system utilized a 5× magnification for image collection.

Flow cytometry protocol

Fresh SVF samples were diluted in PBS. Diluted SVF was mixed with HO/PI solution and the mixture was incubated for 45 min in a 37 °C water bath. CytoCount beads were added the mixture was analyzed on a Synergy Cell Sorter by counting 10,000 beads. The ratio of beads to Hoechst-positive cells (gated on canine peripheral blood mononuclear cells [PBMCs] for cell size) was used to determine the percentage of viable and dead (PI-positive) cells per mL of the SVF sample. The Synergy Cell Sorter utilized an excitation wavelength of 355 and 488 nm for excitation of HO and PI, respectively. The method was performed for the first five samples and the final two individual samples.

Gating protocol for flow cytometry counting

An initial gate was set on paraformaldehyde-fixed canine PBMCs to exclude events that were smaller than PBMCs. The cell size gate was then transferred onto the SVF sample to identify PBMC sized cells. A second gate was set on HO-positive events to identify nucleated cells in the SVF. A third gate was set on PI-negative cells to determine the percent viable cells. Finally, a fourth gate was set on the counting beads so a count of 10,000 beads could be established.

Results

- AO is green, PI is orange, and HO is blue.
- There are numerous cellular debris and non-nucleated particles that can be observed in the brightfield images, which showed weak to no fluorescent signals. It is obvious that if one is to manually count the SVF samples without proper training on counting specification, human error can be introduced.
- The fluorescent images showed bright and dim populations that were used to gate the live, dead, and non-nucleated cells.

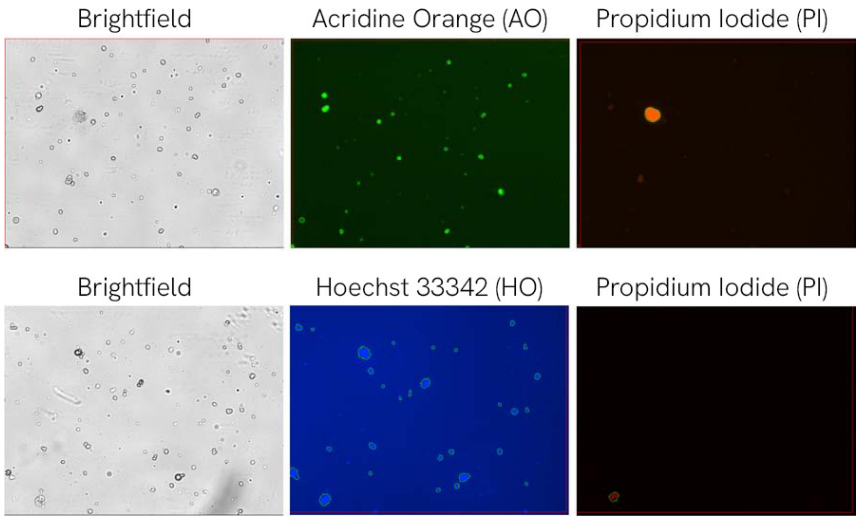

Figure 1: Brightfield and fluorescent images of SVF samples stained with AO/PI and HO/PI.

- The experiment showed comparable concentration values for Sample A- D between all three methods. The deviations were approximately ±10%.
- As for Sample E, the image and flow cytometry method showed good correlation. In contrast, the hemocytometer result was approximately 30% lower, which may indicate the difficulty of manual counting highly concentrated samples (Similar trend shown in Sample D, where hemocytometer result was also lower.)
- Overall, this experiment allowed optimization of image cytometry parameters to measure specific cell particles stained with AO/PI that was comparable to flow cytometry.

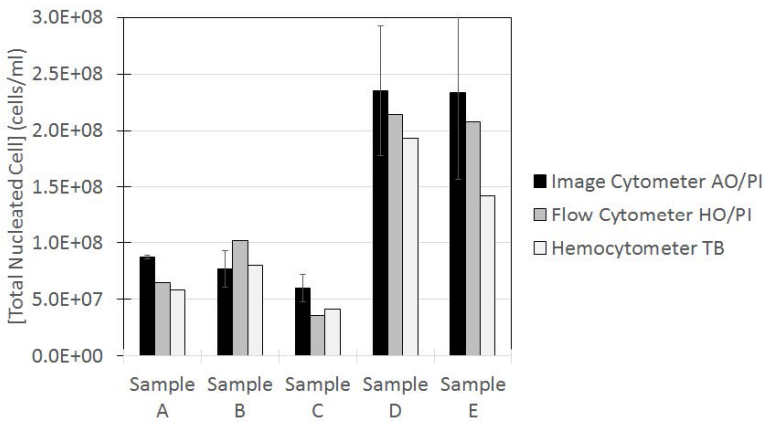

Figure 2: Concentration comparison results of five SVF samples between hemocytometer, image and flow cytometry method.

- Concentrations measured for the two samples were comparable between the three detection methods at a deviation of less than 10%. A two-Sample T-test was conducted. The p-values for AO/PI compared to HO/PI using image and flow cytometry, and manual hemocytometer are all greater than 0.05, meaning that the results are statistically the same.
- In sample 1, the hemocytometer measurement showed ~10% difference compared to image and flow cytometry method, which increased the overall deviation. The increase in cell count could potentially be due to over counting of cellular debris and RBCs.
- Since both image and flow cytometry methods required fluorescent nucleic acid dyes, the results are more comparable, whereas the hemocytometer method generated higher variation. If a comparison is generated between only image and flow cytometry, the deviations for sample 1 and 2 become less than 5% and 2%, respectively.
- A two-Sample T-test was conducted for comparing the detection methods for both samples. The p-values for AO/PI compared to HO/PI using image and flow cytometry are greater than 0.05, which means that the results are statistically the same. However, the TB manual counting method showed a significant reduction in the viability results at ~87 and 83%, where the p-value for AO/PI compared to manual hemocytometer is less than 0.05, meaning that the results are not statistically the same. This reduction may have been due to toxic effects of TB on the viability of cells, which has been shown previously [31].

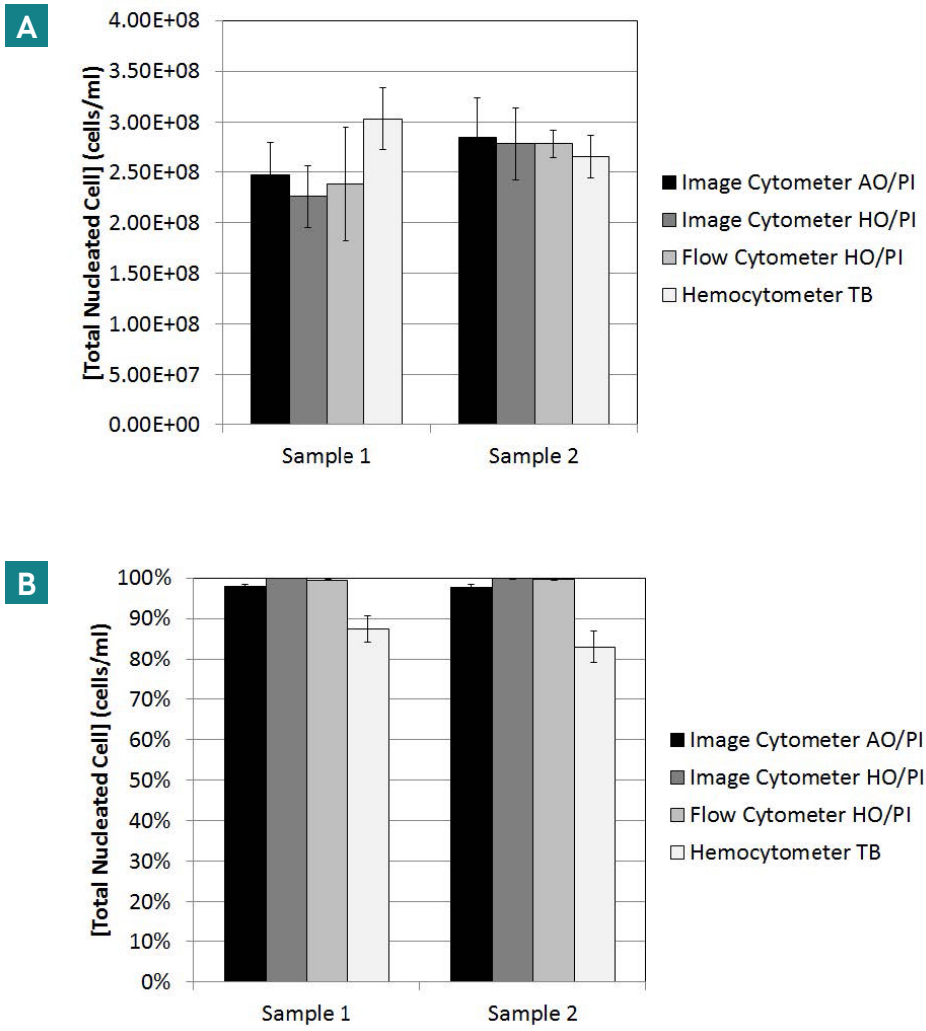

Figure 3: Concentration (A) and viability (B) comparison results between hemocytometer, image and flow cytometry method.

Conclusion

- In conclusion, the concentration and viability measurements using the three detection methods have shown comparable results.
- Viability results from the image cytometer using AO/ PI and HO/PI were highly comparable to the flow cytometer data. Since fluorescent detection methods only stain nucleated cells, debris from adipose tissue does not interfere with viability and concentration counts, which can potentially provide more precise and consistent results in comparison to the manual hemocytometer method.
- The results have validated automated the image cytometry method for accurate SVF sample analysis, which can also improve the efficiency of SVF concentration and viability measurements.
- Further study can be conducted to quantify the changes in SVF cell size or morphological information through automated image-based analysis [13].

References

1. Al Battah, F., et al., *Current status of human adipose-derived stem cells: differentiation into hepatocyte-like cells.* ScientificWorldJournal, 2011. 11: p. 1568-81.
2. Hong, S.J., D.O. Traktuev, and K.L. March, *Therapeutic potential of adipose-derived stem cells in vascular growth and tissue repair.* Curr Opin Organ Transplant, 2010. 15(1): p. 86-91.
3. Kim, S.C., D.J. Han, and J.Y. Lee, *Adipose tissue derived stem cells for regeneration and differentiation into insulin-producing cells.* Curr Stem Cell Res Ther, 2010. 5(2): p. 190-4.
4. Lindroos, B., R. Suuronen, and S. Miettinen, *The potential of adipose stem cells in regenerative medicine.* Stem Cell Rev, 2011. 7(2): p. 269-91.
5. Mazo, M., et al., *Adipose-derived stem cells for myocardial infarction.* J Cardiovasc Transl Res, 2011. 4(2): p. 145-53.
6. Mizuno, H., M. Tobita, and A.C. Uysal, *Concise review: Adipose-derived stem cells as a novel tool for future regenerative medicine.* Stem Cells, 2012. 30(5): p. 804-10.
7. Uysal, A.C. and H. Mizuno, *Tendon regeneration and repair with adipose derived stem cells.* Curr Stem Cell Res Ther, 2010. 5(2): p. 161-7.
8. Zavan, B., et al., *Neural potential of adipose stem cells.* Discov Med, 2010. 10(50): p. 37-43.
9. de Villiers, J.A., N. Houreld, and H. Abrahamse, *Adipose derived stem cells and smooth muscle cells: implications for regenerative medicine.* Stem Cell Rev, 2009. 5(3): p. 256-65.
10. Rada, T., R.L. Reis, and M.E. Gomes, *Adipose tissue-derived stem cells and their application in bone and cartilage tissue engineering.* Tissue Eng Part B Rev, 2009. 15(2): p. 113-25.
11. Hoogendoorn, R.J., et al., *Adipose stem cells for intervertebral disc regeneration: current status and concepts for the future.* J Cell Mol Med, 2008. 12(6A): p. 2205-16.
12. Chan, L.L., et al., *Rapid image-based cytometry for comparison of fluorescent viability staining methods.* J Fluoresc, 2012. 22(5): p. 1301-11.
13. Lo Surdo, J. and S.R. Bauer, *Quantitative approaches to detect donor and passage differences in adipogenic potential and clonogenicity in human bone marrow-derived mesenchymal stem cells.* Tissue Eng Part C Methods, 2012. 18(11): p. 877-89.

Revvity, Inc.
940 Winter Street
Waltham, MA 02451 USA

(800) 762-4000
www.revvity.com